



Characterizing the Retinal Phenotype of the Thy1-h[A30P] α -syn Mouse Model of Parkinson's Disease

Lien Veys^{1,2}, Joyce Devroye^{1,2}, Evy Lefevere^{1,2}, Lien Cools^{1,2}, Marjan Vandenabeele^{1,2} and Lies De Groef^{1,2*}

¹ Research Group of Neural Circuit Development and Regeneration, Department of Biology, KU Leuven, Leuven, Belgium,

² Department of Biomedical Sciences, Leuven Brain Institute, Leuven, Belgium

OPEN ACCESS

Edited by:

Yuyi You,
Macquarie University, Australia

Reviewed by:

Thierry Baron,
Laboratoire de Lyon, Agence
Nationale de Sécurité Sanitaire
de l'Alimentation, de l'Environnement
et du Travail (ANSES), France
Jürgen Winkler,
University of Erlangen Nuremberg,
Germany

*Correspondence:

Lies De Groef
lies.degroef@kuleuven.be

Specialty section:

This article was submitted to
Neurodegeneration,
a section of the journal
Frontiers in Neuroscience

Received: 16 June 2021

Accepted: 19 August 2021

Published: 07 September 2021

Citation:

Veys L, Devroye J, Lefevere E,
Cools L, Vandenabeele M and
De Groef L (2021) Characterizing
the Retinal Phenotype of the
Thy1-h[A30P] α -syn Mouse Model
of Parkinson's Disease.
Front. Neurosci. 15:726476.
doi: 10.3389/fnins.2021.726476

Despite decades of research, disease-modifying treatments of Parkinson's disease (PD), the second most common neurodegenerative disease worldwide, remain out of reach. One of the reasons for this treatment gap is the incomplete understanding of how misfolded alpha-synuclein (α -syn) contributes to PD pathology. The retina, as an integral part of the central nervous system, recapitulates the PD disease processes that are typically seen in the brain, and retinal manifestations have emerged as prodromal symptoms of the disease. The timeline of PD manifestations in the visual system, however, is not fully elucidated and the underlying mechanisms are obscure. This highlights the need for new studies investigating retinal pathology, in order to propel its use as PD biomarker, and to develop validated research models to investigate PD pathogenesis. The present study pioneers in characterizing the retina of the Thy1-h[A30P] α -syn PD transgenic mouse model. We demonstrate widespread α -syn accumulation in the inner retina of these mice, of which a proportion is phosphorylated yet not aggregated. This α -syn expression coincides with inner retinal atrophy due to postsynaptic degeneration. We also reveal abnormal retinal electrophysiological responses. Absence of selective loss of melanopsin retinal ganglion cells or dopaminergic amacrine cells and inflammation indicates that the retinal manifestations in these transgenic mice diverge from their brain phenotype, and questions the specific cellular or molecular alterations that underlie retinal pathology in this PD mouse model. Nevertheless, the observed α -syn accumulation, synapse loss and functional deficits suggest that the Thy1-h[A30P] α -syn retina mimics some of the features of prodromal PD, and thus may provide a window to monitor and study the preclinical/prodromal stages of PD, PD-associated retinal disease processes, as well as aid in retinal biomarker discovery and validation.

Keywords: retina, visual system, alpha-synuclein, transgenic mouse model, Parkinson's disease

Abbreviations: α -syn, Alpha-synuclein; α -syn mice, Thy1-h[A30P] α -syn mice; AQP4, Aquaporin 4; ChAT, Choline acetyltransferase; CNS, Central nervous system; ERG, Electroretinography; DAPI, 4',6-diamidino-2-phenylindole; GCL, Ganglion cell layer; GFAP, Glial fibrillary acidic protein; Iba-1, Ionized calcium-binding adapter molecule 1; INL, Inner nuclear layer; IPL, Inner plexiform layer; NFL, Nerve fiber layer; OP, Oscillatory potential; p- α -syn, Phosphorylated serine-129 α -syn; pSTR, Positive scotopic threshold response; RGC, Retinal ganglion cell; TH, Tyrosine hydroxylase; ThioS, Thioflavin S; WT, Wild type.

INTRODUCTION

Despite decades of research, disease-modifying treatments of Parkinson's disease (PD), the second most common neurodegenerative disease worldwide, remain out of reach (Guo et al., 2018; Veys et al., 2019). It has been suggested that one of the principal reasons for this treatment gap is the lack of accurate and timely diagnosis. Traditionally, diagnosis is based on the cardinal motor symptoms of PD (tremor, rigidity, bradykinesia, and postural instability), which only arise years after a long non-symptomatic phase during which a large proportion of the dopaminergic cells in the substantia nigra are lost (Jankovic, 2008). In order to preserve brain function, therapies -and hence diagnosis- should be focused on the preclinical (asymptomatic) and prodromal (early symptomatic) stages (Forsaa et al., 2010; Mahlknecht et al., 2015; Hustad and Aasly, 2020). In 2017, new diagnostic criteria for PD have been defined by the International Parkinson Disease and Movement Disorders Society (Postuma and Berg, 2017; Marsili et al., 2018), whereby the probability of an individual to develop PD is now calculated based on several predictors, such as age, environmental predictors, prodromal signs, genetic risk variables, and biomarker testing (Postuma et al., 2016). Constant updating of these diagnostic criteria is required as more insights into early stage PD emerge (Postuma and Berg, 2017).

The retina has become a target organ in the search for early biomarkers, relevant diagnostic criteria and techniques that are amenable to population-wide patient screening and disease monitoring. As an integral part of the central nervous system (CNS), the eye can be considered a window to the brain. The visual pathway has shown to be an excellent model system to gain insight into classical neurodegenerative diseases, as both retina and brain are often affected by these diseases and share disease processes (e.g., neurodegeneration, inflammation, aggregation of misfolded proteins, mitochondrial dysfunction; Armstrong, 2009; Martínez-Lapiscina et al., 2014; Rahimi et al., 2015; Veys et al., 2019; Kashani et al., 2021). Therefore, it is not surprising that in many PD patients, one or more visual symptoms are described, such as decreased visual acuity, spatial contrast sensitivity, and color vision (Price et al., 1992; Archibald et al., 2011; Armstrong, 2011; Bodis-Wollner, 2013; Guo et al., 2018). Retinal dysfunction at least partially contributes to these deficits (Bertrand et al., 2012; Mazzarella and Cole, 2016). This is corroborated by retinal imaging via optical coherence tomography (OCT) and with electroretinography (ERG) measurements, which revealed, respectively, retinal nerve fiber layer (NFL), ganglion cell layer (GCL), inner plexiform layer (IPL), and inner nuclear layer (INL) thinning (Shrier et al., 2012; Adam et al., 2013; London et al., 2013; Spund et al., 2013; Lee et al., 2014; Bodis-Wollner et al., 2014b; Boeke et al., 2016; Aydin et al., 2018; Matlach et al., 2018); and abnormalities of the photopic b-wave, scotopic oscillatory potentials (OPs), and P50 component of the pattern ERG in PD patients (Nightingale et al., 1986; Gottlob et al., 1987; Burguera et al., 1990; Ikeda et al., 1994; Peppe et al., 1992, 1995, 1998; Langheinrich et al., 2000; Sartucci et al., 2006; Garcia-Martin et al., 2014; Nowacka et al., 2015; Kashani et al., 2021). Histopathological studies

have revealed pathological manifestations that may underlie these changes in *in vivo* measures, including a reduction in dopamine levels in the retina (Nguyen-Legros, 1988; Harnois and Di Paolo, 1990; Chorostecki et al., 2015), reduced density and complexity of dopaminergic neurons (Ortuño-Lizarán et al., 2020) and melanopsin-positive retinal ganglion cells (RGCs; Ortuno-Lizaran et al., 2018b), and, finally, the presence of alpha-synuclein (α -syn) and phosphorylated (S129) α -syn (p- α -syn) inclusions in the retina (Beach et al., 2014; Ho et al., 2014; Bodis-Wollner et al., 2014a; Ortuno-Lizaran et al., 2018a; Veys et al., 2019). Importantly, p- α -syn deposits in the retina accumulate in parallel with the brain, already during the prodromal stage of PD, and are associated with PD severity (Ortuno-Lizaran et al., 2018a). This reinforces that retinal biomarkers have a high potential for PD diagnosis and disease monitoring.

Further research into the (temporal) relationship between retinal biomarker alterations and neurodegenerative changes in the brain is needed, however, for retinal biomarkers to be adopted in the clinic. Longitudinal and prospective studies in PD patients and patients at risk of developing PD will be essential to assess the value of retinal biomarkers for PD (Kashani et al., 2021). Animal models of PD, on the other hand, can support these studies, by providing a framework in which the correlation between retinal biomarkers and disease manifestations can be explored and novel insights into the molecular and cellular changes underlying the retinal manifestations of PD can be obtained (Santano et al., 2011; Normando et al., 2016; Price et al., 2016; Mammadova et al., 2018, 2021; Veys et al., 2019). Altogether, the wide availability of technologies for non-invasive high-resolution ocular imaging, such as OCT, is a clear advantage over current brain imaging techniques (De Groef and Cordeiro, 2018) and, collectively, visual function measures, ERG, and retinal imaging could offer a multimodal biomarker approach for PD diagnosis, stratification, and monitoring (Guo et al., 2018; Turcano et al., 2018; Veys et al., 2019).

In this study, we aim to fill the need for well-characterized preclinical models to study retinal alternations in PD. We characterized the retinal phenotype of the Thy1-h[A30P] α -syn mouse model, by studying α -syn accumulation, neurodegeneration, inflammation, synaptic integrity, and retinal function. The brain phenotype of this mouse model has been studied before, yet the retinal phenotype remains untouched (Kahle et al., 2000; Neumann et al., 2002; Freichel et al., 2007; Ekmark-Lewen et al., 2018). Here, we used *in vivo* retinal imaging and electrophysiology measurements with high clinical translatability, combined with *post mortem* histological studies, to map the timeline of retinal disease manifestations in these mice.

MATERIALS AND METHODS

Animals

Thy1-h[A30P] α -syn mice (C57BL/6 background, RRID:MG1:2652214) and corresponding wild type (WT) controls, were bred under standard laboratory conditions (Kahle et al., 2000). Both female and male mice were used at 4, 8, 12, 15, and 18 months of age. All experiments were

performed according to the European directive 2010/63/EU and in compliance with protocols approved by the KU Leuven institutional ethical committee.

(Immuno)histochemistry

Prior to eye dissection, mice were euthanized by an intraperitoneal injection of 60 mg/kg sodium pentobarbital (Dolethal, Vetoquinol) followed by transcardial perfusion with saline and 4% paraformaldehyde (PFA). Next, eyes were either fixed in 1% PFA for 4 h at 4°C and embedded in paraffin, or in 4% PFA for 1 h at RT for wholemount preparations. The latter were post-fixed for 1 h in 4% PFA for another hour.

Seven-micrometer sagittal paraffin sections were deparaffinized and stained with hematoxylin (Sigma) and eosin (Sigma) and mounted with Distyrene Plasticizer Xylene mounting medium (Sigma). For Thioflavin S histological staining, sections were stained for 5 min with Thioflavin S (Sigma, 1/200 in 1:1 distilled water and ethanol) and mounted with mowiol (Sigma). For immunohistochemistry, sections were incubated overnight with one or two of the following primary antibodies: human specific α -syn (1/5000; Millipore, clone Syn211 [36-008] RRID:AB_310817), α -syn (1/1000; produced and kindly provided by V. Baekelandt, KU Leuven, for double staining with p- α -syn), p- α -syn (1/5000; Elan Pharmaceuticals), p62 (1/200; Proteintech [#55274-1-AP], RRID:AB_11182278), Brn3a (1/750; Santa Cruz Biotechnology, c-20 [#sc-31984], RRID:AB_2167511), tyrosine hydroxylase (TH; 1/1000; Millipore [#AB152], RRID:AB_390204), choline acetyltransferase (ChAT; 1/100; Millipore [#AB144P], RRID:AB_2079751), VGLUT1 (1/1000, Synaptic Systems [#135 302], RRID:AB_887877), Prox1 (1/500; Biolegend [PCB-238C]), Homer1 (1/500; Synaptic Systems [#160 003], RRID:AB_887730), glial fibrillary acidic protein (GFAP; 1/1000; Dako [#Z0334], RRID:AB_10013382), or aquaporin 4 (AQP4; 1/10000; Alomone labs [AQP-004], RRID:AB_2039734). For α -syn, Brn3a, TH, ChAT, Prox1, and Homer1, antigen retrieval with heated citrate buffer (20 min, 95°C) was used, while no antigen retrieval treatment was used for VGLUT1 and proteinase K (5 min, 20 μ g/ml, Qiagen) antigen retrieval was used for GFAP stainings. Fluorescent labeling was performed using an Alexa-488 labeled secondary antibody (Invitrogen) for Brn3a, TH, ChAT, Prox1, VGLUT1, and GFAP staining, or with a fluorescein or cyanine 3 tyramid signal amplification kit (PerkinElmer) for p- α -syn, α -syn, and Homer1 stainings. Finally, slides were counterstained with 4',6-diamidino-2-phenylindole and mounted with mowiol.

For wholemount immunohistochemistry, tissue permeabilization was achieved by a freeze-thaw step (15 min, -80°C), followed by overnight incubation with one of the following primary antibodies: p- α -syn (1/5000; Elan Pharmaceuticals), TH (1/1000; Millipore [#AB152], RRID:AB_390204), melanopsin (1/5000; Advanced Targeting Systems [#AB-N38], RRID:AB_1608077), or ionized calcium-binding adapter molecule 1 (Iba-1; 1/1000; Wako [#019-19741], RRID:AB_839504). Subsequently, fluorescent labeling was performed using an Alexa-488 labeled secondary antibody (Invitrogen) and wholemounts were mounted with mowiol.

Image Analysis

Imaging was performed using a FV1000 confocal or FV1000-M multiphoton microscope (Olympus) or a conventional epifluorescence microscope (DM6, Leica).

Image analyses were performed with Fiji software (Schindelin et al., 2012). For retinal wholemounts, the entire perimeter of the wholemount was outlined and its area measured prior to analysis. For sections, five sections per mouse were investigated, including the central section containing the optic nerve head, and the sections located 210 and 420 μ m anterior/posterior. On each section, analysis was done over a distance of 300 μ m at four locations per section. For α -syn, TH and GFAP, the immunopositive area was measured in the inner retina (from the retinal NFL until the INL included), while for AQP4 both the outer retina (from OPL to ONL) and inner retina were measured and for VGLUT1 and Homer1, only the IPL was included (Van Hove et al., 2020). For cell counting, both on wholemounts and sections, Fiji "Cell Counter" plugin was used. Microglia density and morphology were quantified as described in Davis et al. (2017) on projection images of z-stack (step size 1.5 μ m) pictures of Iba-1 stained wholemounts (Davis et al., 2017).

Optical Coherence Tomography

Optical coherence tomography imaging was performed as described before (Sergeys et al., 2019; Vandenabeele et al., 2021). Briefly, after pupil dilatation with tropicamide (0.5%, Tropicol, Théa), the retina of anesthetized animals was imaged (1000 A-scans, 100 B-scans, 1.4 \times 1.4 mm, BiopTigen Envisu R2200). Retinal layer thickness was measured using InVivoVue Diver (v 3.0.8, BiopTigen) software, at 16 locations in the central retina spaced around the optic nerve head, and averaged per mouse.

Electroretinography

Electroretinography was performed as described before (Sergeys et al., 2019; Vandenabeele et al., 2021). Full-field flash dark-adapted electroretinograms were measured at increasing flash intensities of 0.003, 0.01, 0.1, 1, 2.5, and 7.5 cd*s/m². Electroretinograms were analyzed using Espion software (v6.59.9, Diagnosys), as shown in **Supplementary Figure 1**. To analyze the OPs on the rising part of the b-wave, a band pass filter (75–300 Hz) was used. The positive scotopic threshold response (pSTR) was measured at 1 \times 10⁻⁴ cd*s/m². 1 week after baseline ERG or pSTR measurement, mice were intraperitoneally injected with benserazide hydrochloride (12.5 g/kg, Sigma) and L-DOPA (25 g/kg, Sigma) 50' and 30' prior to ERG/pSTR measurement, respectively.

Statistical Analysis

Statistical analyses were performed using GraphPad Prism (v8.4.3, GraphPad, RRID:SCR_002798). The number of animals (*n*) used is depicted on the figures and the statistical analyses are indicated in the figure legends. Data are presented as mean \pm SEM. Differences were considered statistically significant for two-sided *p*-values < 0.05 (**p* < 0.05; ***p* < 0.01; ****p* < 0.001; and *****p* < 0.0001).

RESULTS

Retinal Accumulation of (Phosphorylated) α -syn in Thy1-h[A30P] α -syn Mice

α -syn expression, phosphorylation, and aggregation was studied in the retina of WT and Thy1-h[A30P] α -syn mice (α -syn mice) of various ages, using (immuno)stainings for transgenic human α -syn, phosphorylated (serine-129) α -syn (p- α -syn; detecting both human and rodent α -syn), thioflavin S (ThioS) and p62. Conform with previously published data of Veys et al. (2019), h α -syn expression was observed in neuronal cell bodies in the GCL, in neurites in the retinal NFL and IPL and in dispersed cell bodies in the INL of 4-, 8-, 12-, 15-, and 18-month-old Thy1-h[A30P] α -syn mice (Figures 1A–F,T; Veys et al., 2019). The h α -syn positive cell types in the inner retina comprise RGCs, as shown by double staining with Brn3a (Figure 1U), and amacrine cells, based on their morphology and location (Figures 1V–X). Furthermore, the accumulation of h α -syn in dopaminergic, (nor)adrenergic, cholinergic, or AII amacrine cells was ruled out based on the lack of colocalization with TH, ChAT, and Prox1 positive cells, respectively (Figures 1V–X; Müller et al., 2017). Quantitative analysis of the h α -syn fluorescent area did not reveal any progressive changes in h α -syn expression in the inner retina of α -syn mice with aging (Figure 1M). Next, a fraction of α -syn was phosphorylated, most prominently in cell bodies and neurites in the GCL (Figures 1G–L,S,T), and this did not change with age (Figure 1N), not even in end-stage diseased animals with severe signs of hind limb paralysis (data not shown). At 18 months of age, only $34 \pm 8\%$ of strongly α -syn positive cells in the GCL also contained p- α -syn. Finally, we assessed p62 and ThioS labeling to investigate α -syn ubiquitination and aggregation, respectively. At 18 months of age, no p62 accumulation nor relocalization was observed in the retina of α -syn mice as compared to WT mice (Figures 1Q,R), and no ThioS positive aggregates were found in the retina of transgenic nor WT animals (Figures 1O,P). Of note, although no accumulation of ThioS-positive or p62-positive cellular inclusions was detected in the Thy1-h[A30P] α -syn PD mouse model, we cannot exclude that oligomeric, prefibrillar, or non-fibril α -syn conformers contribute to the retinal phenotype observed in these mice (Lashuel et al., 2013; Roberts and Brown, 2015; Cascella et al., 2021). This needs to be explored in follow-up studies.

Altogether, these data show that, while both α -syn overexpression and phosphorylation are present in the retina of Thy1-h[A30P] α -syn mice already at a young age, α -syn aggregation and ubiquitination do not manifest.

Synaptic Degeneration in the Retina of Old Thy1-h[A30P] α -syn Mice

Spectral domain OCT was applied in a longitudinal *in vivo* experiment to measure the thickness of the retinal layers in α -syn mice and WT controls, early in their life (4 and 8 months) and at 12, 15, and 18 months of age (Figures 2A,B,D–F). At 4 months of age, a minor yet significant thickening of the photoreceptor layer (PL) was found in the α -syn mice ($p = 0.0023$; Figure 2A). This

difference in retinal thickness persisted at 12, 15, and 18 months ($p = 0.0009$, $p = 0.0130$, and $p = 0.0122$; Figures 2C–G). Furthermore, at 12 months, α -syn mice also displayed thinning of the IPL, which persisted at 15 and 18 months ($p = 0.0034$ at 12 months, $p = 0.0336$ at 15 months, $p = 0.0444$ at 18 months; Figures 2C–G).

As retinal thinning is typically a sign of neurodegeneration, we next performed a more in-depth analysis of different subpopulations of inner retinal neurons at 15 months of age to clarify the origin of the observed IPL thinning. Given that the IPL consists of neurites emerging from cell bodies in both the GCL and INL, cell density was assessed in these layers on hematoxylin and eosin-stained sections. No overt neurodegeneration was seen in α -syn mice (Figure 2H). Additionally, a detailed analysis of disease-relevant neuronal subtypes, also at 15 months of age, revealed that cell numbers of intrinsically photosensitive RGCs (melanopsin positive) in the GCL and of dopaminergic (TH positive) amacrine cells in the INL (Figures 2I–N) were not affected. However, IPL thinning may also occur due to dendrite or synapse loss, a pathological process that is known to precede loss of neuronal cell bodies. In line with the preservation of dopaminergic cell bodies (cf. above), we found that the dopaminergic plexus of the retina, measured as the TH-immunopositive area in the inner retina, was unaltered in α -syn mice of 15 months of age (Figures 2O–Q). However, taking a closer look at the synaptic integrity of the IPL, via immunostainings with the established pre- and postsynaptic markers VGLUT1 and Homer1, we revealed loss of postsynaptic contacts yet preservation of the presynaptic terminals in 15-month-old transgenic mice (Figures 2R–W). Altogether, these findings suggest that synaptic degeneration in the retina underlies the observed IPL thinning.

Electrophysiological Changes in the Retina of Thy1-h[A30P] α -syn Mice With Aging

In a next series of experiments, we sought to further identify the neuronal cell types that are affected in the α -syn mouse and to establish whether neuronal dysfunction can be detected already at younger ages compared to the OCT thinning that only become apparent at 12 months. Indeed, neuronal death is often preceded by functional changes, and these prodromal manifestations of the disease are of particular interest for biomarker development (Nowacka et al., 2015; Barber et al., 2017; Turcano et al., 2018; Hustad and Aasly, 2020). First, OPs as a read-out for amacrine cell function, were assessed. Already at 4 months, the area under the curve was larger in α -syn mice as compared to WT animals for high intensity light stimuli ($2.5 \text{ cd}^* \text{ s/m}^2$: $p = 0.0137$; $7.5 \text{ cd}^* \text{ s/m}^2$: $p = 0.0094$), and this effect persisted in older transgenic animals of 8 ($1 \text{ cd}^* \text{ s/m}^2$: $p = 0.0191$; $2.5 \text{ cd}^* \text{ s/m}^2$: $p = 0.0452$; $7.5 \text{ cd}^* \text{ s/m}^2$: $p = 0.0050$), 12 ($1 \text{ cd}^* \text{ s/m}^2$: $p = 0.0034$; $2.5 \text{ cd}^* \text{ s/m}^2$: $p = 0.0039$; $7.5 \text{ cd}^* \text{ s/m}^2$: $p = 0.0023$), and 18 months of age ($1 \text{ cd}^* \text{ s/m}^2$: $p = 0.0001$; Figures 3A,B and Supplementary Figure 1F). Second, we measured RGC function via the pSTR. Not yet at 4 months, but at 8, 12, and 18 months, the pSTR latency time was shorter in α -syn mice as compared to WT controls

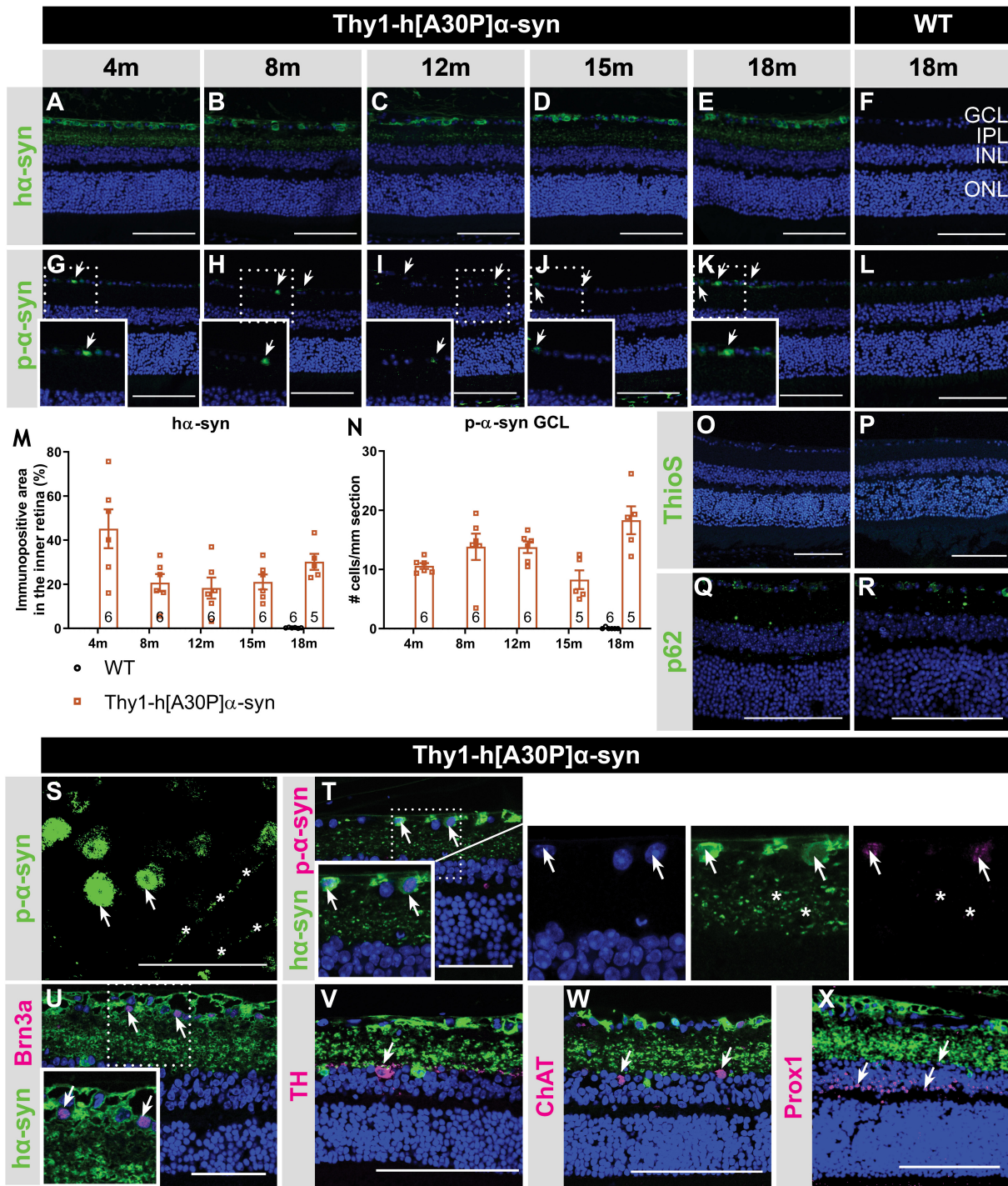


FIGURE 1 | Inner retinal ha-syn expression is accompanied by α -syn phosphorylation, yet no ThioS positive aggregation or p62 accumulation, in the retina of Thy1-h[A30P] α -syn mice. Representative images of ha-syn immunostainings (A–E); p- α -syn immunostainings (G–K); and ThioS staining (O) on retinal sections of α -syn mice at 4, 8, 12, 15 and 18 months of age. (F,L,P) No staining was observed in the WT controls, at any age (only 18 months shown here). (M,N) Quantitative analysis of the ha-syn fluorescent area and counting of the p- α -syn positive cells did not reveal an increase of ha-syn expression in the inner retina or p- α -syn cell density in α -syn mice with age. (O,P) No ThioS positive inclusions were found in the retina of transgenic nor wild type animals in any of the age groups. (Q,R) No difference in retinal p62 accumulation or localization was detected between transgenic and wild type animals at 18 months of age. (S) p- α -syn immunostaining on a retinal wholemount of an α -syn mouse showed p- α -syn localization in cell bodies (arrows) and neurites (asterisks). (T) Double staining of ha-syn with p- α -syn revealed clear colocalization. (U–X) Double staining of ha-syn with Brn3a, TH, ChAT and Prox1 revealed expression of Brn3a in ha-syn positive cells, yet no colocalization in dopaminergic and cholinergic cells. Scale bar: 100 μ m (A–R, V–X) or 50 μ m (S–U); GCL, ganglion cell layer; INL, inner nuclear layer; IPL, inner plexiform layer; and ONL, outer nuclear layer.

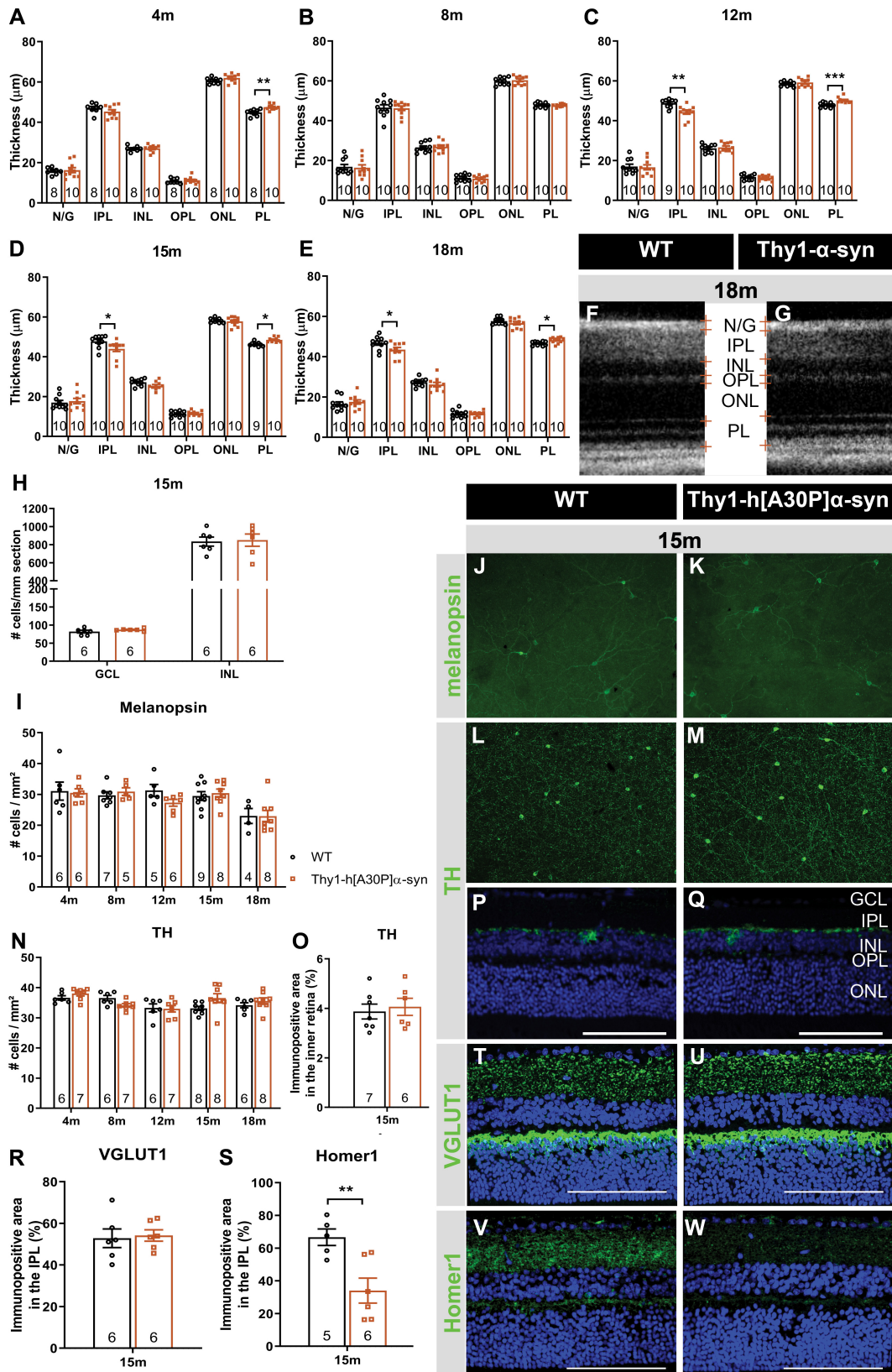


FIGURE 2 | Continued

FIGURE 2 | Outer retinal thickening and inner retinal thinning, associated with loss of postsynaptic labeling, in Thy1-h[A30P] α -syn mice. **(A–E)** Longitudinal OCT measurements in 4- **(A)**, 8- **(B)**, 12- **(C)**, 15- **(D)**, and 18-month-old **(E–G)** mice, revealed significant differences in retinal layer thickness between α -syn and WT mice of 4 months (PL thickening), 15 months (PL thickening and IPL thinning), and 12 and 18 months of age (PL thickening and IPL thinning). **(H)** Cell counts on hematoxylin and eosin-stained sections in the GCL and in the INL did not reveal significant differences between transgenic animals and WT controls at 15 months of age. **(I–W)** Representative images of retinal wholemounts stained for melanopsin **(J,K)** and TH **(L,M)**, and of retinal sections stained for TH **(P,Q)**, VGLUT1 **(T,U)**, and Homer-1 **(V,W)**, of 15-month-old α -syn and WT mice. Counting the number of melanopsin- **(I)** and TH- **(N)** positive cells on retinal wholemounts revealed no significant differences between transgenic and WT animals. No significant differences were uncovered in TH plexus **(O)** and VGLUT1 **(R)** immunopositive area, yet a strong decrease of the Homer1 **(S)** signal was seen. Scale bar: 100 μ m; Two-Way ANOVA with Tukey multiple comparisons *post hoc* test **(I–N)**. Unpaired *t*-test (per retinal layer; **A–F,O,R,S**); * $p < 0.05$; ** $p < 0.01$; and *** $p < 0.001$. N/G, retinal nerve fiber layer + GCL; GCL, ganglion cell layer; INL, inner nuclear layer; IPL, inner plexiform layer; ONL, outer nuclear layer; OPL, outer plexiform layer; and PL, photoreceptor layer.

($p = 0.0082$ at 8 months, $p = 0.0119$ at 12 months, and $p = 0.0006$ at 18 months; **Figures 3D–F** and **Supplementary Figure 1G**). *a*- and *b*-wave measurements were unaltered, indicating normal functioning of the photoreceptors, bipolar cells, and Müller glia (**Supplementary Figures 1B–E**).

In PD patients, visual defects have been attributed to malfunctioning of the dopaminergic retinal neurons -which constitute a subtype of amacrine cells-, which is supported by the fact that ERG abnormalities can be alleviated by L-DOPA treatment (Ikeda et al., 1994; Djamgoz et al., 1997; Peppe et al., 1998; Turcano et al., 2018). Hence, we assessed the effect of systemic L-DOPA treatment 30 min prior to the ERG measurement in a second, independent study. We found that L-DOPA did not fully reverse the effects of genotype on the OPs in 8-month-old mice, nor the pSTR latency in 18-month-old mice (**Figures 3C,F**). These findings are in line with the absence of dopaminergic degeneration as observed in the immunohistological studies (*cfr.* above). Overall, ERG changes in the α -syn mice suggest that amacrine cells and RGCs become dysfunctional with age, yet TH immunostainings showed that it is unlikely that a selective loss of dopaminergic neurons underlies this phenotype.

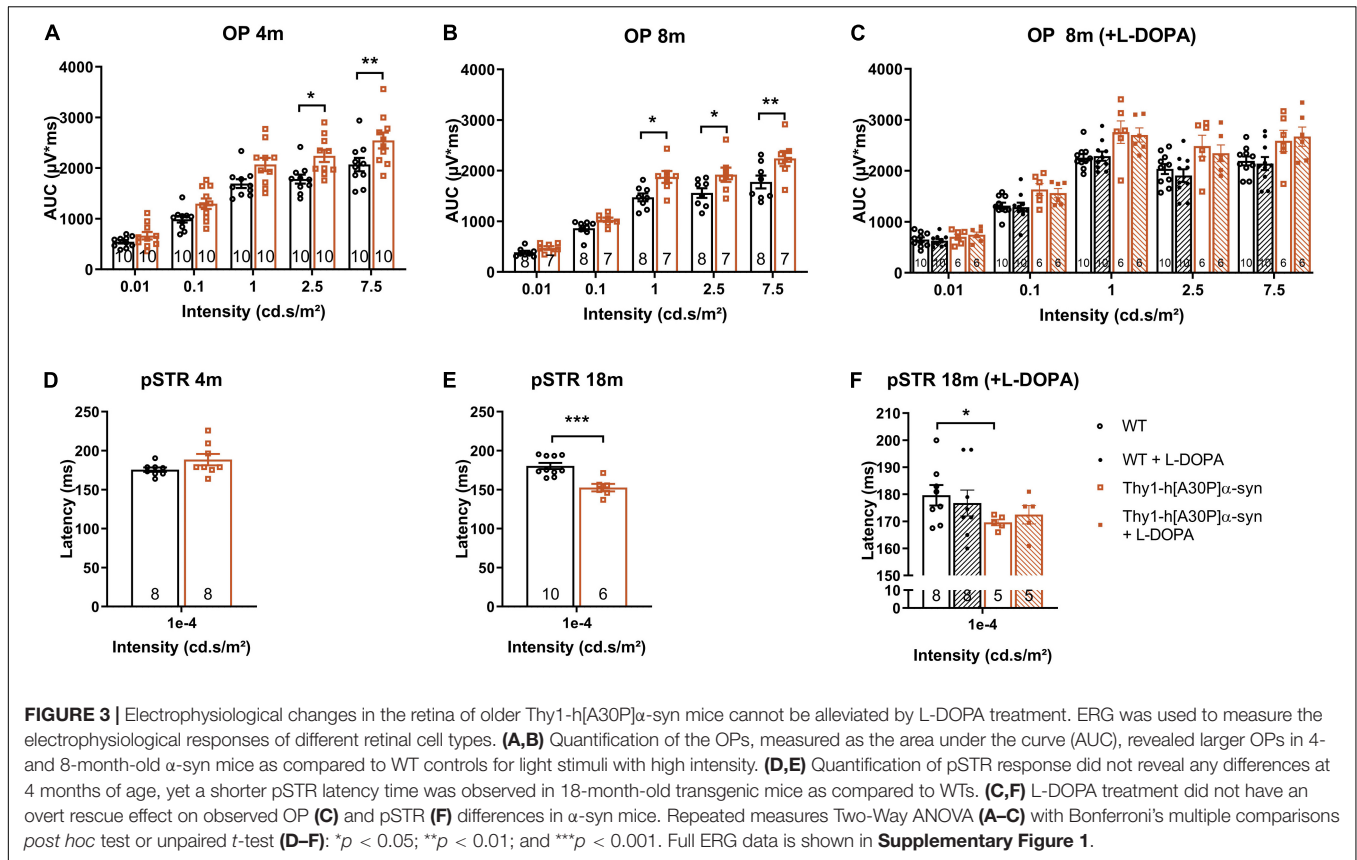
No Signs of Neuroinflammation in the Retina of Thy1-h[A30P] α -syn Mice

Previous studies demonstrated that α -syn triggers neuroinflammation, and that, in turn, inflammation increases α -syn phosphorylation and pathology in synucleinopathies (Lee et al., 2010; Tansey and Goldberg, 2010; Ramirez et al., 2017; Ferreira and Romero-Ramos, 2018). Furthermore, retinal inflammation has been linked to both swelling of the outer retina and ERG deviations, and may therefore underlie -at least in part- the OCT and ERG abnormalities that we observed in the Thy1-h[A30P] α -syn mice (Mirza and Jampol, 2013; Petzold, 2016; Pisa et al., 2021; Xia et al., 2021). Hence, we next investigated macroglia and microglia reactivity and water homeostasis in the retina. First, Müller glia and astrocytes were investigated. Analysis of GFAP immunostainings on retinal cross-sections of α -syn versus WT mice did not reveal differences in immunofluorescent area at 4, 8, 12, 15, and 18 months of age and radial fiber density at 15 months of age between the two genotypes, although an expected aging effect was present (**Figures 4A–D**). Second, the cause of outer retinal swelling was further investigated by measuring the expression of AQP4 (**Figures 4G,H**). AQP4 is a water channel expressed

by the Müller glia, of which differences in expression levels and cellular localization have been linked to retinal edema and neuroinflammation (Amann et al., 2016). In AD patients, it was found to be overexpressed in the brain and associated with blood-brain barrier disruption (Foglio and Luigi Fabrizio, 2010; Fukuda and Badaut, 2012). However, no genotypic difference in immunofluorescent area nor localization in the inner versus outer retinal layers was revealed in mice of 15 months old (**Figures 4E,F**). Third, microgliosis was investigated on retinal wholemounts stained for Iba-1 (**Figures 4J,K,M,N**). Cell density did not differ in transgenic versus WT mice at any of the selected ages (**Figure 4I**). Furthermore, we investigated cell morphology, to probe for changes in soma roundness as a sign of microglia reactivity (Davis et al., 2017). However, no difference in cell body roundness of Iba-1⁺ cells was observed between the two genotypes (**Figure 4L**). In conclusion, this data suggests that retinal inflammation nor edema underlie the OCT and ERG abnormalities that we observed in the α -syn mice.

DISCUSSION

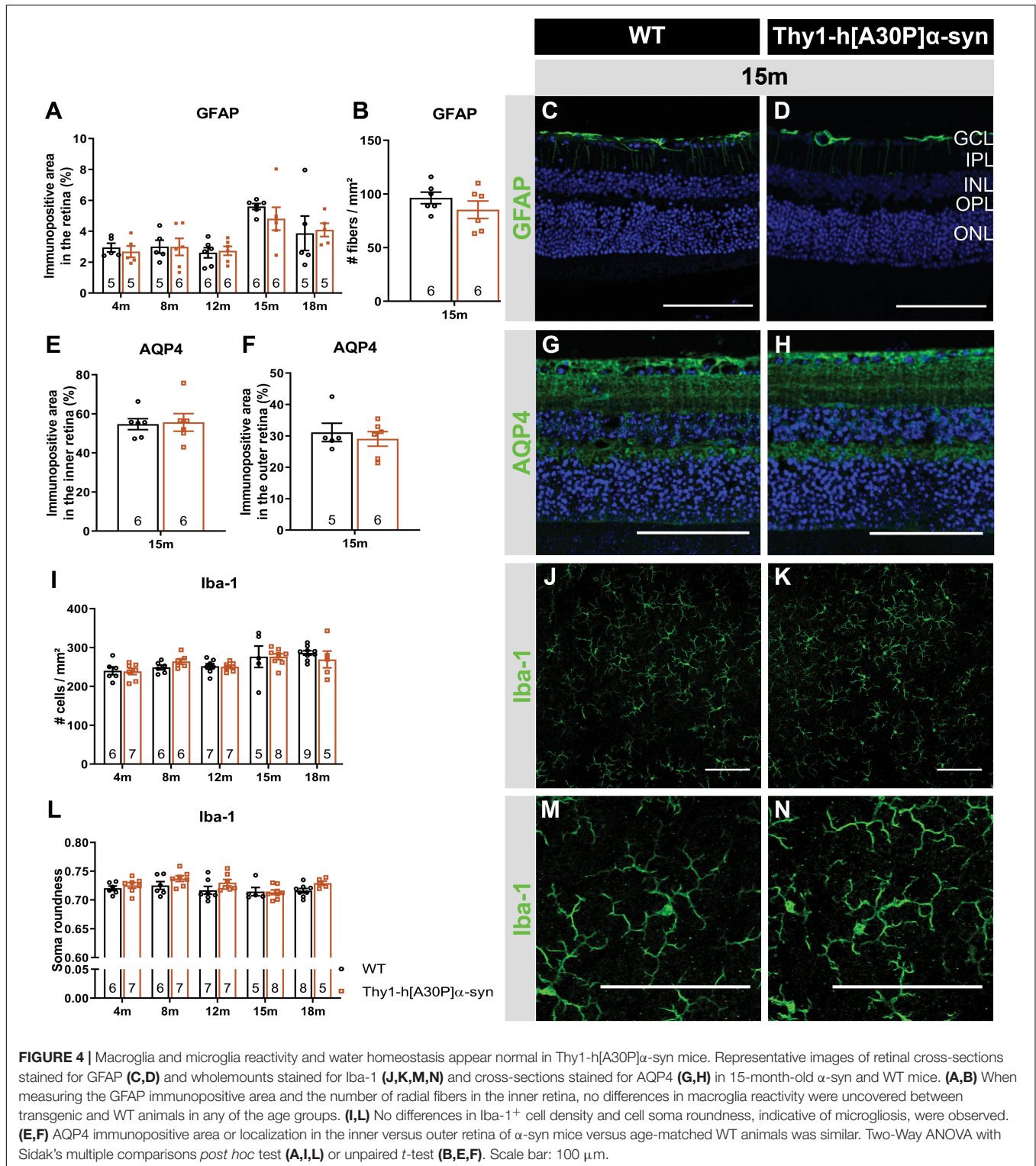
In recent years, neurodegenerative disease research is increasingly focusing on the pre- and early symptomatic stages of disease, when the cascade of neurodegenerative events has only just started and a sufficiently large pool of neurons still remains that can be rescued with disease-modifying treatments to preserve brain function. To identify and take opportunity of this early time window for treatment, however, novel biomarkers and inexpensive, minimally invasive, and widely available screening and diagnostic tests are needed. These may be found in the retina. As an integral part of the CNS, the retina recapitulates many of the PD-related neurodegenerative process in the brain. Indeed, a multitude of OCT and ERG studies has shown that neuronal dysfunction and degeneration affects the retina of PD patients (Garcia-Martin et al., 2014; Boeke et al., 2016; Aydin et al., 2018; Veys et al., 2019). Furthermore, accumulating evidence of retinal dopamine deficits and α -syn misfolding suggest that this is the result of the same disease processes that also drive neurodegeneration in the brain (Guo et al., 2018; Ortuno-Lizaran et al., 2018a; Veys et al., 2019; Ortuño-Lizarán et al., 2020). It remains to be explored, however, what the correlation between the PD manifestations in the brain and retina is, and whether the mechanisms behind these manifestations are the same. A deeper understanding of this will be essential for the rational use of retinal biomarkers for



PD diagnosis, monitoring and/or stratification, and will also aid research into novel retinal biomarkers. Animal research will remain an essential complement to the extensive clinical studies that are obviously needed, offering flexibility in study subjects and read-outs to dig into the cellular and molecular changes that characterize the PD retina and dictate the retinal biomarker results. Up till now, multiple studies have investigated the brain phenotype of PD animal models, yet retinal manifestations have received little attention (Santano et al., 2011; Normando et al., 2016; Price et al., 2016; Veys et al., 2019). Mammadova et al. investigated the retinal phenotype of the TgM83 mouse model. This transgenic mouse is characterized by α -syn accumulation mainly in the outer retina and p- α -syn pathology in both outer and inner retina, and thereby only partially mimics the inner retina pathology seen in PD patients (Mammadova et al., 2018, 2021). In addition, and in contrast to the Thy1-h[A30P] α -syn model, neuroinflammation, and photoreceptor cell loss were seen in the TgM83 model, again partially reflecting human disease – where also microglia reactivity was seen (Tansey and Goldberg, 2010; Ferreira and Romero-Ramos, 2018; Mammadova et al., 2018). Both in the Thy1-h[A30P] α -syn and TgM83 mice, and in contrast to reports on the human PD retina (Archibald et al., 2009; Mammadova et al., 2018; Ortuño-Lizarán et al., 2020), TH immunoreactivity was unaltered (**Table 1**). The lack of dopaminergic degeneration, even in end-stage animals (data not shown), highlights the limitations of the available transgenic mouse models in recapitulating the full complexity of human

disease. Of note, this is in line with findings in the brain, where a lack of progressive neurodegeneration has been reported for several rodent PD models (Lim and Ng, 2009; Dawson et al., 2010; Kin et al., 2019). Furthermore, the diverging retinal manifestations observed in these two mouse models might result from the use of distinct promoters (Thy1 versus Prp) and/or different mutated forms of α -syn (A30P versus A53T), which might influence the aggregation process (Flagmeier et al., 2016). By examining the retina of the Thy1-h[A30P] α -syn PD mouse model, we aim to establish a research model with a retinal α -syn expression pattern that more closely resembles α -synucleinopathy in PD patients. We believe that such a model is valuable to investigate the retina-brain connection in PD and thereby propel retinal biomarker discovery and validation research and fundamental studies of the role of α -syn in health and disease.

We revealed that, from a young age onward, α -syn overexpression can be observed in the inner retina of α -syn mice, alongside a fraction of phosphorylated α -syn in RGC neurites and somata; an observation that complies with previously described (p)- α -syn localization in the retina of PD patients (**Table 1**; Ortuño-Lizarán et al., 2018a; Veys et al., 2019). Despite the lack of ThioS positive protein aggregates and accumulation of the Lewy body marker p62, α -syn overexpression did result in thinning of the inner retina in α -syn mice from the age of 12 months, similar to the inner retinal remodeling seen in PD patients (**Table 1**; Shrier et al., 2012; Adam et al., 2013;



Spund et al., 2013; Lee et al., 2014; Bodis-Wollner et al., 2014b). Our data revealed that neurodegeneration of dopaminergic amacrine cells or melanopsin positive RGCs cannot account for this IPL thinning uncovered with OCT imaging. Instead, synapse loss may underlie this retinal atrophy. Indeed, significant

changes in the density of Homer1+ postsynaptic -yet not VGLUT1+ presynaptic- terminals in the IPL underscore the OCT alterations. Postsynaptic terminals in the IPL come from RGCs and amacrine cells, neurons for which we also observed α -syn overexpression and abnormal ERG responses (Connaughton,

TABLE 1 | Summary of the phenotypical alterations observed in the retina of PD patients, Thy1-h[A30P] α -syn mice.

| PD patients | References | Thy1-h[A30P] α -syn mice | TgM83 mice |
|---|---|---|--|
| α -syn in GCL, IPL, and INL | Beach et al., 2014; Ho et al., 2014; Bodis-Wollner et al., 2014a | α -syn in GCL, IPL, and INL | α -syn in ONL and INL |
| p- α -syn positive cell bodies and neurites in GCL | Beach et al., 2014; Ortuno-Lizaran et al., 2018a | p- α -syn positive cell bodies and neurites in GCL | p- α -syn labeling in outer and inner retina p-Tau (Thr231) in OPL and GCL |
| Thinning of NFL, GCL, IPL, and INL (OCT) | Shrier et al., 2012; Adam et al., 2013; Spund et al., 2013; Lee et al., 2014; Bodis-Wollner et al., 2014b; Matlach et al., 2018 | Thinning of IPL (OCT) | Thinning of ONL (histology) |
| Decreased TH levels and TH-positive cell density in INL Decreased TH + plexus complexity | Nguyen-Legros, 1988; Harnois and Di Paolo, 1990; Chorostecki et al., 2015; Ortuno-Lizaran et al., 2020 | Preserved TH-positive cell density in INL Preserved TH + plexus size in IPL | Preserved TH levels in INL |
| Decreased melanopsin-positive cell density in GCL and dendritic tree complexity | Ortuno-Lizaran et al., 2018b | Preserved melanopsin-positive cell density in GCL | |
| Increased microglial reactivity (Iba-1) | Doorn et al., 2014; Ferreira and Romero-Ramos, 2018 | No microglial reactivity (Iba-1) | Increased microglial reactivity (CD11b, CD68) |
| No macroglial reactivity (GFAP) | Mirza et al., 1999 | No macroglial reactivity (GFAP) | Macroglial reactivity (GFAP) |
| RGC, bipolar and amacrine cell dysfunction (ERG): – diminished responses of the photopic b-wave, scotopic oscillatory potentials and P50 component of the pattern ERG reversed by L-DOPA – reversed by L-DOPA | Nightingale et al., 1986; Gottlob et al., 1987; Burguera et al., 1990; Ikeda et al., 1994; Peppe et al., 1992, 1995, 1998; Langheinrich et al., 2000; Sartucci et al., 2006; Garcia-Martin et al., 2014; Nowacka et al., 2015; Kashani et al., 2021 | RGC and amacrine cell dysfunction (ERG): – supernormal responses of the scotopic oscillatory potentials and pSTR (starting at 4 and 8 months, respectively) – no overt response to L-DOPA | |

Retinal manifestations on the TgM83 mouse model were described in Mammadova et al. (2018). OCT, optical coherence tomography; NFL, nerve fiber layer; GCL, ganglion cell layer; IPL, inner plexiform layer; INL, inner nuclear layer; ONL, outer nuclear layer; OPL, outer plexiform layer; PL, photoreceptor layer; ERG, electroretinography; OPs, oscillatory potentials; pSTR, positive scotopic threshold response; and TH: tyrosine hydroxylase.

1995). Furthermore, synapse loss has been shown to occur early in the neurodegenerative process, for example in the retina of glaucoma models and patients, or in the brain of AD or PD models and patients (Selkoe, 2002; Della Santina et al., 2013; Purro et al., 2014; Bellucci et al., 2016; Subramanian and Tremblay, 2021). More specifically, a decrease in synaptic volume in of pre- and post-synapses has been reported in the striatum of PD patients (Bellucci et al., 2016; Reeve et al., 2018; Gcwenza et al., 2021). Of note, an age-related decrease of postsynaptic retinal proteins was also observed in the plexiform layers of *Octodon degus*, the only rodent with naturally occurring AD (Chang et al., 2020).

The retinal atrophy and synapse loss observed in α -syn mice is accompanied by functional alterations, which were uncovered using ERG. These were striking for several reasons. First, amacrine cell responses were supernormal in α -syn mice. Although abnormal OPs are also typically seen in PD patients, these ERG alterations tend to decrease rather than increase in human patients (Table 1; Gottlob et al., 1987; Burguera et al., 1990; Ikeda et al., 1994; Nowacka et al., 2015). Remarkably, these supernormal ERG responses in α -syn mice coincide with a thickening of the PL, which might be caused by local edema or swelling of the photoreceptors (Devos et al., 2005; Archibald et al., 2009). Interestingly, this outer retinal swelling was also seen in the early disease stages of a rotenone-induced PD rat model, where it was suggested to be linked to increased mitochondrial biogenesis in the highly energy demanding photoreceptor cells

(Normando et al., 2016). Outer retinal thickening has also been observed to co-occur with supernormal ERG measurements in the retina of the 3 \times Tg-AD Alzheimer's (Chiquita et al., 2019a). Furthermore, both supernormal scotopic ERG measurements and PL layer thickening have been related to a mild inflammatory phenotype in the early stages of retinal pathology linked to multiple sclerosis (Mirza and Jampol, 2013; Petzold, 2016). Yet, with the measurements used in this study, no abnormalities in AQP4 water channels and no inflammatory response of the macro- and microglia was detected. Second, an equally striking observation in this study is the increased conduction velocity of RGC electrophysiological responses in older animals, reminiscent of the RGC hyperactivity in early AD disease stages of 5 \times FAD mice (Araya et al., 2021). In AD models, amyloid-beta overproduction can lead to neuronal network hyperexcitability (Kazim et al., 2021). As AD and PD are both neurodegenerative proteinopathies and amyloid-beta and α -syn biology show many parallels, one could hypothesize that similar neuronal network hyperexcitability events might occur in PD too (Goedert, 2015). This hypothesis is supported by our data on synaptic integrity, which show preservation of presynaptic integrity yet loss of postsynaptic density. The postsynaptic density Homer1 proteins link metabotropic glutamate receptors to intracellular effectors, mediating the glutamate inducible effects in postsynaptic RGCs and amacrine cells (Connaughton, 1995). Dysregulation of extracellular glutamate concentrations at the synapse can lead to excess release of glutamate, which

is known to induce hyperexcitability in postsynaptic neurons (Gasparini and Griffiths, 2013). An alternative explanation for the supernormal ERG responses by RGCs might relate to the physiological role of α -syn at the synapse, where it is suggested to associate with synaptic vesicles and to influence neurotransmitter release (Sulzer and Edwards, 2019). Since α -syn overexpression inhibits synaptic vesicle exocytosis, one could hypothesize that decreased exocytosis might disturb the tightly maintained balance that is involved in synaptic regulation (Sulzer and Edwards, 2019). Finally, the electrophysiological alterations observed in this study were, in contrast to ERG changes in PD patients, not reversed by L-DOPA treatment

(Table 1; Archibald et al., 2009). Along with the observed lack of dopaminergic cell loss in the retina and the absence of α -syn in dopaminergic amacrine cells in the α -syn mice, this suggests a dopamine-independent mechanism underlying the ERG alterations. Which neuronal subtype(s) account for the observed electrophysiological abnormalities should be elucidated in future research via more advanced electrophysiology studies, e.g., using patch clamping or microelectrode arrays (Obien et al., 2015; Chiquita et al., 2019b).

Besides generating insights into the (patho)physiological role of α -syn and the disease processes that lead to the retinal PD phenotype, we postulate that the α -syn mouse may also aid the

TABLE 2 | Overview of the reported phenotypical alterations in the brain and spinal cord of Thy1-h[A30P] α -syn mice, in relation to observations in the retina.

| Observations in the brain and spinal cord | Time point of first observation | References | Own observations in the retina | Time point of first observation |
|--|---------------------------------|---|---|---------------------------------|
| Functional read-outs | | | | |
| Decreased fine motor performance (beam transversal test) | 2 months, worsens with age | Ekmark-Lewen et al., 2018 | | |
| Lower general activity and more risk-taking (multivariate concentric square field test) | 8 months | Ekmark-Lewen et al., 2018 | | |
| Impaired spatial learning and memory (Morris water maze) | 12 months | Freichel et al., 2007 | | |
| Impaired fear conditioning (freezing behavior after foot shock) | 12 months | Freichel et al., 2007 | | |
| Higher locomotor activity | 12 months | Freichel et al., 2007 | | |
| Impaired motor behavior (rotarod test) | 17 months | Freichel et al., 2007 | | |
| (Hind limb) paralysis | 18 months | Freichel et al., 2007 | | |
| Premature death | 18 months | Freichel et al., 2007 | | |
| Decreased frequency of spontaneous excitatory postsynaptic currents (electrophysiology) | 1 month | Chesselet et al., 2012 | OP alterations (ERG) | 4 months |
| | | | pSTR latency alterations (ERG) | 18 months |
| Histopathology | | | | |
| α -syn overexpression in neuronal cell bodies and neurites in the brain and spinal cord | 6 month | Kahle et al., 2000 | α -syn overexpression in neuronal cell bodies and neurites in the inner retina | 4 months |
| p- α -syn positive neurons in spinal cord and brainstem | 1 months | Freichel et al., 2007 | p- α -syn positive neurons in GCL | 4 months |
| Oligomeric α -syn in brainstem, midbrain and hippocampus | 8 months | Ekmark-Lewen et al., 2018 | | |
| PK-resistant α -syn in brain | 9 months | Neumann et al., 2002; Freichel et al., 2007 | | |
| Ubiquitin-positive inclusions in pontine reticular nuclei and ventral horn of the spinal cord | 12 months | Neumann et al., 2002 | | |
| ThioS reactive species in brainstem | 16 months | Schell et al., 2009 | No ThioS reactivity detected | |
| Decreased TH immunoreactivity in central midbrain regions | 8 months | Ekmark-Lewen et al., 2018 | No changes in TH immunoreactivity | |
| Increased GFAP immunoreactivity in brainstem | 8 months | Neumann et al., 2002; Ekmark-Lewen et al., 2018 | No changes in GFAP immunoreactivity | |
| Limited inflammatory response (increase in Mac2 ⁺ immune cells) | 8 months | Ekmark-Lewen et al., 2018 | No changes in Iba-1 immunoreactivity | |
| No reports of neurodegeneration | | | PL thickening (OCT) | 4 months |
| | | | IPL thinning (OCT) | 15 months |

OCT, optical coherence tomography; PL, photoreceptor layer; IPL, inner plexiform layer; INL, inner nuclear layer; ERG, electroretinography; OPs, oscillatory potentials; pSTR, positive scotopic threshold response; TH, tyrosine hydroxylase; PK, proteinase K; and ThioS, thioflavin S.

understanding of the retina-brain connection. Indeed, the α -syn mouse is characterized by h α -syn overexpression in neuronal cell bodies and neurites in the brain and spinal cord (Table 2; Kahle et al., 2000; Freichel et al., 2007) and p- α -syn and oligomeric α -syn were detected in brainstem, midbrain, and hippocampus of 8-month-old transgenic mice. In addition, older mice also develop proteinase K-resistant α -syn deposits, ubiquitin-positive neuritic and cell body inclusions, and ThioS reactive α -syn species in various CNS regions (Table 2; Neumann et al., 2002; Schell et al., 2009). This synucleinopathy in the brain is accompanied by astrogliosis and dopaminergic neurodegeneration (Ekmark-Lewen et al., 2018), and led to a variety of behavioral changes in fine motor performance, learning, and memory, finally leading to paralysis and premature death around the age of 18 months (Table 2; Freichel et al., 2007; Ekmark-Lewen et al., 2018). We conclude that the rather subtle retinal phenotype stands in marked contrast to findings in the brain of these mice, exposing the organotypic heterogeneity of the retina compared to other brain structures. Notably, this heterogeneity may be exploited as a strength in future research, and aid the understanding of disease mechanisms and selective vulnerability in different locations in the CNS.

Irrespective of the differences in the retina versus brain phenotype of the α -syn mice, this study highlights the potential of the retina for *in vivo* imaging and electrophysiology measurements with non-invasive techniques, such as OCT and ERG. Especially OCT, which detected retinal thinning in the inner retina in our transgenic mice similar to what has been described in the human PD retina, has the potential to become a low-cost, non-invasive tool for diagnosis and follow-up of PD disease progression (Shrier et al., 2012; Adam et al., 2013; Spund et al., 2013; Lee et al., 2014; Bodis-Wollner et al., 2014b). Importantly, these techniques have the advantage of being suitable for both patient and preclinical research, thereby providing relevant endpoint measures and enhancing the translatability of this research to the clinic.

In conclusion, this study uncovered morphological and electrophysiological abnormalities in the α -syn mouse retina. While this mouse model does not display dopaminergic neurodegeneration or neuroinflammation, its retina is characterized by a decreased density of postsynaptic terminals that may reflect neurotransmitter dysregulation and as such is linked to the observed ERG changes and IPL thinning. These pathological changes resemble the loss of synapses and neuronal dysfunction that are typically observed during the earliest stages of neurodegenerative diseases and are in line with a multitude of OCT and ERG studies in PD patients and animal models. The methodologies and the α -syn mouse model used

in this study thus constitute a toolbox for research of the early, preclinical/prodromal stages of PD, and may aid fundamental research of PD-associated retinal disease processes, such as α -syn mediated synaptic dysfunction, as well as retinal biomarker discovery and validation.

DATA AVAILABILITY STATEMENT

The raw data supporting the conclusions of this article will be made available by the authors, without undue reservation.

ETHICS STATEMENT

The animal study was reviewed and approved by KU Leuven institutional ethical committee.

AUTHOR CONTRIBUTIONS

LV and LD contributed to the conception of the study, elaborated on the study design, and wrote the manuscript. LV, JD, EL, LC, and MV performed the experimental work. LC edited the manuscript. All authors have read and approved the manuscript.

FUNDING

LV, MV, and LD are supported by the Research Foundation Flanders (fellowships 1S51718N, 1190320N, and 12I3817N). The funders had no role in study design, data collection and analysis, decision to publish, or preparation of the manuscript.

ACKNOWLEDGMENTS

We acknowledge support from Research Foundation Flanders (fellowships to LV, MV, and LD). We like to express our sincere thanks to Philipp J. Kahle for donating the Thy1-h[A30P] α -syn mice, and to Isabelle Etienne and Tine Van Bergen (Oxurion NV, Leuven, Belgium) for assistance with tissue processing.

SUPPLEMENTARY MATERIAL

The Supplementary Material for this article can be found online at: <https://www.frontiersin.org/articles/10.3389/fnins.2021.726476/full#supplementary-material>

REFERENCES

- Adam, C. R., Shrier, E., Ding, Y., Glazman, S., and Bodis-Wollner, I. (2013). Correlation of inner retinal thickness evaluated by spectral-domain optical coherence tomography and contrast sensitivity in Parkinson disease. *J. Neuro Ophthalmol.* 33, 137–142. doi: 10.1097/WNO.0b013e31828c4e1a
- Amann, B., Kleinwort, K. J. H., Hirmer, S., Sekundo, W., Kremmer, E., Hauck, S. M., et al. (2016). Expression and distribution pattern of aquaporin 4, 5 and 11 in retinas of 15 different species. *Int. J. Mol. Sci.* 17:1145. doi: 10.3390/ijms17071145
- Araya, J., Bello, F., Shivashankar, G., Neira, D., Durán-Aniotz, C., Acosta, M. L., et al. (2021). Retinal ganglion cells functional changes in a mouse model of Alzheimer's disease are linked with neurotransmitter alterations. *J. Alzheimers Dis.* 82, S5–S18. doi: 10.3233/jad-201195
- Archibald, N. K., Clarke, M. P., Mosimann, U. P., and Burn, D. J. (2009). The retina in Parkinson's disease. *Brain* 132, 1128–1145. doi: 10.1093/brain/awp068

- Archibald, N. K., Clarke, M. P., Mosimann, U. P., and Burn, D. J. (2011). Visual symptoms in Parkinson's disease and Parkinson's disease dementia. *Mov. Disord.* 26, 2387–2395. doi: 10.1002/mds.23891
- Armstrong, R. A. (2009). Alzheimer's disease and the eye. *J. Optom.* 2, 103–111. doi: 10.3921/joptom.2009.103
- Armstrong, R. A. (2011). Visual symptoms in Parkinson's disease. *Parkinson Dis.* 2011:908306. doi: 10.4061/2011/908306
- Aydin, T. S., Umit, D., Nur, O. M., Fatih, U., Asena, K., Nefise, O. Y., et al. (2018). Optical coherence tomography findings in Parkinson's disease. *Kaohsiung J. Med. Sci.* 34, 166–171. doi: 10.1016/j.kjms.2017.11.006
- Barber, T. R., Klein, J. C., Mackay, C. E., and Hu, M. T. M. (2017). Neuroimaging in pre-motor Parkinson's disease. *NeuroImage Clin.* 15, 215–227. doi: 10.1016/j.nicl.2017.04.011
- Beach, T. G., Carew, J., Serrano, G., Adler, C. H., Shill, H. A., Sue, L. I., et al. (2014). Phosphorylated alpha-synuclein-immunoreactive retinal neuronal elements in Parkinson's disease subjects. *Neurosci. Lett.* 571, 34–38. doi: 10.1016/j.neulet.2014.04.027
- Bellucci, A., Mercuri, N. B., Venneri, A., Faustini, G., Longhena, F., Pizzi, M., et al. (2016). Parkinson's disease: from synaptic loss to connectome dysfunction. *Neuropathol. Appl. Neurobiol.* 42, 77–94. doi: 10.1111/nan.12297
- Bertrand, J. A., Bedetti, C., Postuma, R. B., Monchi, O., Genier Marchand, D., Jubault, T., et al. (2012). Color discrimination deficits in Parkinson's disease are related to cognitive impairment and white-matter alterations. *Mov. Disord.* 27, 1781–1788. doi: 10.1002/mds.25272
- Bodis-Wollner, I. (2013). Foveal vision is impaired in Parkinson's disease. *Parkinsonism Relat. Disord.* 19, 1–14. doi: 10.1016/j.parkreldis.2012.07.012
- Bodis-Wollner, I., Kozlowski, P. B., Glazman, S., and Miri, S. (2014a). alpha-synuclein in the inner retina in Parkinson disease. *Ann. Neurol.* 75, 964–966. doi: 10.1002/ana.24182
- Bodis-Wollner, I., Miri, S., and Glazman, S. (2014b). Venturing into the no-man's land of the retina in Parkinson's disease. *Mov. Disord.* 29, 15–22. doi: 10.1002/mds.25741
- Boeke, A., Rosen, D., Mastrianni, J., Xie, T., and Bernard, J. (2016). Optical coherence tomography as potential biomarker in Parkinson's disease and Alzheimer's disease (P5.177). *Neurology* 86(16 Suppl.):P5.177.
- Burguera, J. A., Vilela, C., Traba, A., Ameave, Y., and Vallet, M. (1990). [The electroretinogram and visual evoked potentials in patients with Parkinson's disease]. *Arch. Neurobiol.* 53, 1–7.
- Cascella, R., Chen, S. W., Bigi, A., Camino, J. D., Xu, C. K., Dobson, C. M., et al. (2021). The release of toxic oligomers from α -synuclein fibrils induces dysfunction in neuronal cells. *Nat. Commun.* 12:1814. doi: 10.1038/s41467-021-21937-3
- Chang, L. Y. L., Ardiles, A. O., Tapia-Rojas, C., Araya, J., Inestrosa, N. C., Palacios, A. G., et al. (2020). Evidence of synaptic and neurochemical remodeling in the retina of aging degus. *Front. Neurosci.* 14:161. doi: 10.3389/fnins.2020.00161
- Chesselet, M. F., Richter, F., Zhu, C., Magen, I., Watson, M. B., and Subramaniam, S. R. (2012). A progressive mouse model of Parkinson's disease: the Thy1-Syn ("Line 61") mice. *Neurotherapeutics* 9, 297–314. doi: 10.1007/s13311-012-0104-2
- Chiquita, S., Campos, E. J., Castelhana, J., Ribeiro, M., Sereno, J., Moreira, P. I., et al. (2019a). Retinal thinning of inner sub-layers is associated with cortical atrophy in a mouse model of Alzheimer's disease: a longitudinal multimodal in vivo study. *Alzheimers Res. Ther.* 11:90. doi: 10.1186/s13195-019-0542-8
- Chiquita, S., Rodrigues-Neves, A. C., Baptista, F. I., Carecho, R., Moreira, P. I., Castelo-Branco, M., et al. (2019b). The retina as a window or mirror of the brain changes detected in Alzheimer's disease: critical aspects to unravel. *Mol. Neurobiol.* 56, 5416–5435. doi: 10.1007/s12035-018-1461-6
- Chorostecki, J., Seraji-Bozorgzad, N., Shah, A., Bao, F., Bao, G., George, E., et al. (2015). Characterization of retinal architecture in Parkinson's disease. *J. Neurol. Sci.* 355, 44–48. doi: 10.1016/j.jns.2015.05.007
- Connaughton, V. (1995). *Glutamate and Glutamate Receptors in the Vertebrate Retina*. Salt Lake City, UT: University of Utah Health Sciences Center.
- Davis, B. M., Salinas-Navarro, M., Cordeiro, M. F., Moons, L., and De Groef, L. (2017). Characterizing microglia activation: a spatial statistics approach to maximize information extraction. *Sci. Rep.* 7:1576. doi: 10.1038/s41598-017-01747-8
- Dawson, T. M., Ko, H. S., and Dawson, V. L. (2010). Genetic animal models of Parkinson's disease. *Neuron* 66:646. doi: 10.1016/J.NEURON.2010.04.034
- De Groef, L., and Cordeiro, M. F. (2018). Is the eye an extension of the brain in central nervous system disease? *J. Ocul. Pharmacol. Ther.* 34, 129–133. doi: 10.1089/jop.2016.0180
- Della Santina, L., Inman, D. M., Lupien, C. B., Horner, P. J., and Wong, R. O. L. (2013). Differential progression of structural and functional alterations in distinct retinal ganglion cell types in a mouse model of glaucoma. *J. Neurosci.* 33, 17444–17457. doi: 10.1523/JNEUROSCI.5461-12.2013
- Devos, D., Tir, M., Maurage, C. A., Waucquier, N., Defebvre, L., Defoort-Dhellemmes, S., et al. (2005). ERG and anatomical abnormalities suggesting retinopathy in dementia with Lewy bodies. *Neurology* 65, 1107–1110. doi: 10.1212/01.wnl.0000178896.44905.33
- Djamgoz, M. B., Hankins, M. W., Hirano, J., and Archer, S. N. (1997). Neurobiology of retinal dopamine in relation to degenerative states of the tissue. *Vision Res.* 37, 3509–3529. doi: 10.1016/s0042-6989(97)00129-6
- Doorn, K. J., Moors, T., Drukarch, B., van de Berg, W. D. J., Lucassen, P. J., and van Dam, A. M. (2014). Microglial phenotypes and toll-like receptor 2 in the substantia nigra and hippocampus of incidental Lewy body disease cases and Parkinson's disease patients. *Acta Neuropathol. Commun.* 2, 1–17. doi: 10.1186/s40478-014-0090-1
- Ekmekci-Lewen, S., Lindstrom, V., Gumucio, A., Ihse, E., Behere, A., Kahle, P. J., et al. (2018). Early fine motor impairment and behavioral dysfunction in (Thy1)-h[A30P] alpha-synuclein mice. *Brain Behav.* 8:e00915. doi: 10.1002/brb3.915
- Ferreira, S. A., and Romero-Ramos, M. (2018). Microglia response during Parkinson's disease: alpha-synuclein intervention. *Front. Cell. Neurosci.* 12:247. doi: 10.3389/fncel.2018.00247
- Flagmeier, P., Meisl, G., Vendruscolo, M., Knowles, T. P. J., Dobson, C. M., Buell, A. K., et al. (2016). Mutations associated with familial Parkinson's disease alter the initiation and amplification steps of α -synuclein aggregation. *Proc. Natl. Acad. Sci. U.S.A.* 113, 10328–10333. doi: 10.1073/PNAS.1604645113
- Foglio, E., and Luigi Fabrizio, R. (2010). Aquaporins and neurodegenerative diseases. *Curr. Neuropharmacol.* 8, 112–121. doi: 10.2174/157015910791233150
- Forsaa, E. B., Larsen, J. P., Wentzel-Larsen, T., and Alves, G. (2010). What predicts mortality in Parkinson disease? A prospective population-based long-term study. *Neurology* 75, 1270–1276. doi: 10.1212/WNL.0b013e3181f61311
- Freichel, C., Neumann, M., Ballard, T., Muller, V., Woolley, M., Ozmen, L., et al. (2007). Age-dependent cognitive decline and amygdala pathology in alpha-synuclein transgenic mice. *Neurobiol. Aging* 28, 1421–1435. doi: 10.1016/j.neurobiolaging.2006.06.013
- Fukuda, A. M., and Badaut, J. (2012). Aquaporin 4: a player in cerebral edema and neuroinflammation. *J. Neuroinflammation* 9:279. doi: 10.1186/1742-2094-9-279
- Garcia-Martin, E., Rodriguez-Mena, D., Satue, M., Almarcegui, C., Dolz, I., Alarcia, R., et al. (2014). Electrophysiology and optical coherence tomography to evaluate Parkinson disease severity. *Investig. Ophthalmol. Vis. Sci.* 55, 696–705. doi: 10.1167/iovs.13-13062
- Gasparini, C. F., and Griffiths, L. R. (2013). The biology of the glutamatergic system and potential role in migraine. *Int. J. Biomed. Sci.* 9, 1–8.
- Gwensan, N. Z., Russell, D. L., Cowell, R. M., and Volpicelli-Daley, L. A. (2021). Molecular mechanisms underlying synaptic and axon degeneration in Parkinson's disease. *Front. Cell. Neurosci.* 15:44. doi: 10.3389/fncel.2021.626128
- Goedert, M. (2015). NEURODEGENERATION. Alzheimer's and Parkinson's diseases: the prion concept in relation to assembled Abeta, tau, and alpha-synuclein. *Science* 349:1255555. doi: 10.1126/science.1255555
- Gottlob, I., Schneider, E., Heider, W., and Skrandies, W. (1987). Alteration of visual evoked potentials and electroretinograms in Parkinson's disease. *Electroencephalogr. Clin. Neurophysiol.* 66, 349–357. doi: 10.1016/0013-4694(87)90032-0
- Guo, L., Normando, E. M., Shah, P. A., De Groef, L., and Cordeiro, M. F. (2018). Oculo-visual abnormalities in Parkinson's disease: possible value as biomarkers. *Mov. Disord.* 33, 1390–1406. doi: 10.1002/mds.27454
- Harnois, C., and Di Paolo, T. (1990). Decreased dopamine in the retinas of patients with Parkinson's disease. *Investig. Ophthalmol. Vis. Sci.* 31, 2473–2475.
- Ho, C. Y., Troncoso, J. C., Knox, D., Stark, W., and Eberhart, C. G. (2014). Beta-amyloid, phospho-tau and alpha-synuclein deposits similar to those in the brain are not identified in the eyes of Alzheimer's and Parkinson's disease patients. *Brain Pathol.* 24, 25–32. doi: 10.1111/bpa.12070

- Hustad, E., and Aasly, J. O. (2020). Clinical and imaging markers of prodromal Parkinson's disease. *Front. Neurol.* 11:395. doi: 10.3389/fneur.2020.00395
- Ikeda, H., Head, G. M., and Ellis, C. J. (1994). Electrophysiological signs of retinal dopamine deficiency in recently diagnosed Parkinson's disease and a follow up study. *Vision Res.* 34, 2629–2638. doi: 10.1016/0042-6989(94)90248-8
- Jankovic, J. (2008). Parkinson's disease: clinical features and diagnosis. *J. Neurol. Neurosurg. Psychiatry* 79, 368–376. doi: 10.1136/jnnp.2007.131045
- Kahle, P. J., Neumann, M., Ozmen, L., Muller, V., Jacobsen, H., Schindzielorz, A., et al. (2000). Subcellular localization of wild-type and Parkinson's disease-associated mutant alpha-synuclein in human and transgenic mouse brain. *J. Neurosci.* 20, 6365–6373. doi: 10.1523/jneurosci.20-17-06365.2000
- Kashani, A. H., Asanad, S., Chan, J. W., Singer, M. B., Zhang, J., Sharifi, M., et al. (2021). Past, present and future role of retinal imaging in neurodegenerative disease. *Prog. Retin. Eye Res.* 83:100938. doi: 10.1016/j.preteyeres.2020.100938
- Kazim, S. F., Seo, J. H., Bianchi, R., Larson, C. S., Sharma, A., Wong, R. K. S., et al. (2021). Neuronal network excitability in Alzheimer's disease: the puzzle of similar versus divergent roles of amyloid β and tau. *Environ. Health Perspect.* 129:157001. doi: 10.1289/ehp.2020.157001
- Kin, K., Yasuhara, T., Kameda, M., and Date, I. (2019). Animal models for Parkinson's disease research: Trends in the 2000s. *Int. J. Mol. Sci.* 20 doi: 10.3390/ijms20215402
- Langheinrich, T., Tebartz Van Elst, L., Lagrèze, W. A., Bach, M., Lücking, C. H., and Greenlee, M. W. (2000). Visual contrast response functions in Parkinson's disease: evidence from electroretinograms, visually evoked potentials and psychophysics. *Clin. Neurophysiol.* 111, 66–74. doi: 10.1016/S1388-2457(99)00223-0
- Lashuel, H. A., Overk, C. R., Oueslati, A., and Masliah, E. (2013). The many faces of alpha-synuclein: from structure and toxicity to therapeutic target. *Nat. Rev. Neurosci.* 14, 38–48. doi: 10.1038/nrn3406
- Lee, H. J., Suk, J. E., Patrick, C., Bae, E. J., Cho, J. H., Rho, S., et al. (2010). Direct transfer of α -synuclein from neuron to astroglia causes inflammatory responses in synucleinopathies. *J. Biol. Chem.* 285, 9262–9272. doi: 10.1074/jbc.M109.081125
- Lee, J. Y., Kim, J. M., Ahn, J., Kim, H. J., Jeon, B. S., and Kim, T. W. (2014). Retinal nerve fiber layer thickness and visual hallucinations in Parkinson's disease. *Mov. Disord.* 29, 61–67. doi: 10.1002/mds.25543
- Lim, K. L., and Ng, C. H. (2009). Genetic models of Parkinson disease. *Biochim. Biophys. Acta Mol. Basis Dis.* 1792, 604–615. doi: 10.1016/j.bbadis.2008.10.005
- London, A., Benhar, I., and Schwartz, M. (2013). The retina as a window to the brain—from eye research to CNS disorders. *Nat. Rev. Neurol.* 9, 44–53. doi: 10.1038/nrneuro.2012.227
- Mahlknecht, P., Seppi, K., and Poewe, W. (2015). The concept of prodromal Parkinson's disease. *J. Parkinsons. Dis.* 5, 681–697. doi: 10.3233/JPD-150685
- Mammadova, N., Baron, T., Verchère, J., Greenlee, J. J., and Greenlee, M. H. W. (2021). "Retina as a model to study in vivo transmission of α -synuclein in the A53T mouse model of Parkinson's disease," in *Mouse Genetics. Methods in Molecular Biology*, Vol. 2224, eds S. R. Singh, R. M. Hoffman, and A. Singh (New York, NY: Humana), 75–85. doi: 10.1007/978-1-0716-1008-4_5
- Mammadova, N., Summers, C. M., Kokemuller, R. D., He, Q., Ding, S., Baron, T., et al. (2018). Accelerated accumulation of retinal alpha-synuclein (pSer129) and tau, neuroinflammation, and autophagic dysregulation in a seeded mouse model of Parkinson's disease. *Neurobiol. Dis.* 121, 1–16. doi: 10.1016/j.nbd.2018.09.013
- Marsili, L., Rizzo, G., and Colosimo, C. (2018). Diagnostic criteria for Parkinson's disease: from James Parkinson to the concept of prodromal disease. *Front. Neurol.* 9:156. doi: 10.3389/fneur.2018.00156
- Martínez-Lapiscina, E. H., Sanchez-Dalmau, B., Fraga-Pumar, E., Ortiz-Perez, S., Tercero-Urbe, A. I., Torres-Torres, R., et al. (2014). The visual pathway as a model to understand brain damage in multiple sclerosis. *Mult. Scler.* 20, 1678–1685. doi: 10.1177/1352458514542862
- Matlach, J., Wagner, M., Malzahn, U., Schmidtman, I., Steigerwald, F., Musacchio, T., et al. (2018). Retinal changes in Parkinson's disease and glaucoma. *Parkinsonism Relat. Disord.* 56, 41–46. doi: 10.1016/j.parkreldis.2018.06.016
- Mazzarella, J., and Cole, J. (2016). All eyes on neurodegenerative diseases. *Rev. Optom.* 153, 42–52.
- Mirza, B., Hadberg, H., Thomsen, P., and Moos, T. (1999). The absence of reactive astrocytosis is indicative of a unique inflammatory process in Parkinson's disease. *Neuroscience* 95, 425–432. doi: 10.1016/S0306-4522(99)00455-8
- Mirza, R. G., and Jampol, L. M. (2013). *White Spot Syndromes and Related Diseases*. Retin. 5th Edn, 1337–1380. doi: 10.1016/B978-1-4557-0737-9.00076-X
- Müller, L. P. D. S., Azar, S. S., de los Santos, J., and Brecha, N. C. (2017). Prox1 is a marker for AII amacrine cells in the mouse retina. *Front. Neuroanat.* 11:39. doi: 10.3389/FNANA.2017.00039
- Neumann, M., Kahle, P. J., Giasson, B. I., Ozmen, L., Borroni, E., Spooen, W., et al. (2002). Misfolded proteinase K-resistant hyperphosphorylated alpha-synuclein in aged transgenic mice with locomotor deterioration and in human alpha-synucleinopathies. *J. Clin. Invest.* 110, 1429–1439. doi: 10.1172/jci15777
- Nguyen-Legros, J. (1988). Functional neuroarchitecture of the retina: hypothesis on the dysfunction of retinal dopaminergic circuitry in Parkinson's disease. *Surg. Radiol. Anat.* 10, 137–144. doi: 10.1007/bf02307822
- Nightingale, S., Mitchell, K. W., and Howe, J. W. (1986). Visual evoked cortical potentials and pattern electroretinograms in Parkinson's disease and control subjects. *J. Neurol. Neurosurg. Psychiatry* 49, 1280–1287. doi: 10.1136/jnnp.49.11.1280
- Normando, E. M., Davis, B. M., De Groef, L., Nizari, S., Turner, L. A., Ravindran, N., et al. (2016). The retina as an early biomarker of neurodegeneration in a rotenone-induced model of Parkinson's disease: evidence for a neuroprotective effect of rosiglitazone in the eye and brain. *Acta Neuropathol. Commun.* 4:86. doi: 10.1186/s40478-016-0346-z
- Nowacka, B., Lubiński, W., Honczarenko, K., Potemkowski, A., and Safranow, K. (2015). Bioelectrical function and structural assessment of the retina in patients with early stages of Parkinson's disease (PD). *Doc. Ophthalmol.* 131, 95–104. doi: 10.1007/s10633-015-9503-0
- Obien, M. E. J., Deligkaris, K., Bullmann, T., Bakkum, D. J., and Frey, U. (2015). Revealing neuronal function through microelectrode array recordings. *Front. Neurosci.* 9:423. doi: 10.3389/fnins.2014.00423
- Ortuno-Lizaran, I., Beach, T. G., Serrano, G. E., Walker, D. G., Adler, C. H., and Cuenca, N. (2018a). Phosphorylated alpha-synuclein in the retina is a biomarker of Parkinson's disease pathology severity. *Mov. Disord.* 33, 1315–1324. doi: 10.1002/mds.27392
- Ortuno-Lizaran, I., Esquivá, G., Beach, T. G., Serrano, G. E., Adler, C. H., Lax, P., et al. (2018b). Degeneration of human photosensitive retinal ganglion cells may explain sleep and circadian rhythms disorders in Parkinson's disease. *Acta Neuropathol. Commun.* 6:90. doi: 10.1186/s40478-018-0596-z
- Ortuño-Lizarán, I., Sánchez-Sáez, X., Lax, P., Serrano, G. E., Beach, T. G., Adler, C. H., et al. (2020). Dopaminergic retinal cell loss and visual dysfunction in Parkinson disease. *Ann. Neurol.* 88, 893–906. doi: 10.1002/ana.25897
- Pepe, A., Stanzione, P., Pierantozzi, M., Semprini, R., Bassi, A., Santilli, A. M., et al. (1998). Does pattern electroretinogram spatial tuning alteration in Parkinson's disease depend on motor disturbances or retinal dopaminergic loss? *Electroencephalogr. Clin. Neurophysiol.* 106, 374–382. doi: 10.1016/s0013-4694(97)00075-8
- Pepe, A., Stanzione, P., Pierelli, F., De Angelis, D., Pierantozzi, M., and Bernardi, G. (1995). Visual alterations in de novo Parkinson's disease: pattern electroretinogram latencies are more delayed and more reversible by levodopa than are visual evoked potentials. *Neurology* 45, 1144–1148. doi: 10.1212/WNL.45.6.1144
- Pepe, A., Stanzione, P., Pierelli, F., Stefano, E., Rizzo, P. A., Tagliati, M., et al. (1992). Low contrast stimuli enhance PERG sensitivity to the visual dysfunction in Parkinson's disease. *Electroencephalogr. Clin. Neurophysiol.* 82, 453–457. doi: 10.1016/0013-4694(92)90051-i
- Petzold, A. (2016). Retinal glymphatic system: an explanation for transient retinal layer volume changes? *Brain* 139, 2816–2819. doi: 10.1093/brain/aww239
- Pisa, M., Croese, T., Dalla Costa, G., Guerrieri, S., Huang, S. C., Finardi, A., et al. (2021). Subclinical anterior optic pathway involvement in early multiple sclerosis and clinically isolated syndromes. *Brain* 144, 848–862. doi: 10.1093/brain/awaa458
- Postuma, R. B., and Berg, D. (2017). The new diagnostic criteria for Parkinson's disease. *Int. Rev. Neurobiol.* 132, 55–78. doi: 10.1016/bs.irn.2017.01.008
- Postuma, R. B., Berg, D., Adler, C. H., Bloem, B. R., Chan, P., Deuschl, G., et al. (2016). The new definition and diagnostic criteria of Parkinson's disease. *Lancet Neurol.* 15, 546–548. doi: 10.1016/S1474-4422(16)00116-2

- Price, D. L., Rockenstein, E., Mante, M., Adame, A., Overk, C., Spencer, B., et al. (2016). Longitudinal live imaging of retinal alpha-synuclein::GFP deposits in a transgenic mouse model of Parkinson's disease/dementia with Lewy bodies. *Sci. Rep.* 6:29523. doi: 10.1038/srep29523
- Price, M. J., Feldman, R. G., Adelberg, D., and Kayne, H. (1992). Abnormalities in color vision and contrast sensitivity in Parkinson's disease. *Neurology* 42, 887–890. doi: 10.1212/wnl.42.4.887
- Purro, S. A., Galli, S., and Salinas, P. C. (2014). Dysfunction of Wnt signaling and synaptic disassembly in neurodegenerative diseases. *J. Mol. Cell Biol.* 6, 75–80. doi: 10.1093/jmcb/mjt049
- Rahimi, J., Milenkovic, I., and Kovacs, G. G. (2015). Patterns of Tau and alpha-synuclein pathology in the visual system. *J. Parkinsons Dis.* 5, 333–340. doi: 10.3233/JPD-140485
- Ramirez, A. I., de Hoz, R., Salobarra-Garcia, E., Salazar, J. J., Rojas, B., Ajoy, D., et al. (2017). The role of microglia in retinal neurodegeneration: Alzheimer's disease, Parkinson, and Glaucoma. *Front. Aging Neurosci.* 9:214. doi: 10.3389/fnagi.2017.00214
- Reeve, A. K., Grady, J. P., Cosgrave, E. M., Bennison, E., Chen, C., Hepplewhite, P. D., et al. (2018). Mitochondrial dysfunction within the synapses of substantia nigra neurons in Parkinson's disease. *NPJ Parkinsons Dis.* 4:9. doi: 10.1038/s41531-018-0044-6
- Roberts, H. L., and Brown, D. R. (2015). Seeking a mechanism for the toxicity of oligomeric α -synuclein. *Biomolecules* 5:282. doi: 10.3390/Biom5020282
- Santano, C., Perez de Lara, M., and Pintor, J. (2011). "Retinal disturbances in patients and animal models with Huntington's, Parkinson's and Alzheimer's disease," in *Oxidative Stress in Applied Basic Research and Clinical Practice – Studies on Experimental Models*, eds S. Basu and L. Wiklund (New York, NY: Humana Press), 221–250. doi: 10.1007/978-1-60761-956-7_10
- Sartucci, F., Orlandi, G., Bonuccelli, U., Borghetti, D., Murri, L., Orsini, C., et al. (2006). Chromatic pattern-reversal electroretinograms (ChPERGs) are spared in multiple system atrophy compared with Parkinson's disease. *Neurol. Sci.* 26, 395–401. doi: 10.1007/s10072-006-0522-1
- Schell, H., Hasegawa, T., Neumann, M., and Kahle, P. J. (2009). Nuclear and neuritic distribution of serine-129 phosphorylated α -synuclein in transgenic mice. *Neuroscience* 160, 796–804. doi: 10.1016/j.neuroscience.2009.03.002
- Schindelin, J., Arganda-Carreras, I., Frise, E., Kaynig, V., Longair, M., Pietzsch, T., et al. (2012). Fiji: an open-source platform for biological-image analysis. *Nat. Methods* 9, 676–682. doi: 10.1038/nmeth.2019
- Selkoe, D. J. (2002). Alzheimer's disease is a synaptic failure. *Science* 298, 789–791. doi: 10.1126/science.1074069
- Sergeys, J., Etienne, I., Van Hove, I., Lefevre, E., Stalmans, I., Feyen, J. H. M., et al. (2019). Longitudinal in vivo characterization of the streptozotocin-induced diabetic mouse model: focus on early inner retinal responses. *Investig. Ophthalmol. Vis. Sci.* 60, 807–822. doi: 10.1167/iovs.18-25372
- Shrier, E. M., Adam, C. R., Spund, B., Glazman, S., and Bodis-Wollner, I. (2012). Intercular asymmetry of foveal thickness in Parkinson disease. *J. Ophthalmol.* 2012:728457. doi: 10.1155/2012/728457
- Spund, B., Ding, Y., Liu, T., Selesnick, I., Glazman, S., Shrier, E. M., et al. (2013). Remodeling of the fovea in Parkinson disease. *J. Neural Transm.* 120, 745–753. doi: 10.1007/s00702-012-0909-5
- Subramanian, J., and Tremblay, M. È. (2021). Editorial: synaptic loss and neurodegeneration. *Front. Cell. Neurosci.* 15:681029. doi: 10.3389/fncel.2021.681029
- Sulzer, D., and Edwards, R. H. (2019). The physiological role of α -synuclein and its relationship to Parkinson's disease. *J. Neurochem.* 150, 475–486. doi: 10.1111/jnc.14810
- Tansey, M. G., and Goldberg, M. S. (2010). Neuroinflammation in Parkinson's disease: its role in neuronal death and implications for therapeutic intervention. *Neurobiol. Dis.* 37, 510–518. doi: 10.1016/j.nbd.2009.11.004
- Turcano, P., Chen, J. J., Bureau, B. L., and Savica, R. (2018). Early ophthalmologic features of Parkinson's disease: a review of preceding clinical and diagnostic markers. *J. Neurol.* 266, 2103–2111. doi: 10.1007/s00415-018-9051-0
- Van Hove, I., De Groef, L., Boeckx, B., Modave, E., Hu, T. T., Beets, K., et al. (2020). Single-cell transcriptome analysis of the Akimba mouse retina reveals cell-type-specific insights into the pathobiology of diabetic retinopathy. *Diabetologia* 63, 2235–2248. doi: 10.1007/s00125-020-05218-0
- Vandenabeele, M., Veys, L., Lemmens, S., Hadoux, X., Gelders, G., Masin, L., et al. (2021). The App NL-G-F mouse retina is a site for preclinical Alzheimer's disease diagnosis and research. *Acta Neuropathol. Commun.* 9:6. doi: 10.1186/s40478-020-01102-5
- Veys, L., Vandenabeele, M., Ortuno-Lizaran, I., Baekelandt, V., Cuenca, N., Moons, L., et al. (2019). Retinal alpha-synuclein deposits in Parkinson's disease patients and animal models. *Acta Neuropathol.* 137, 379–395. doi: 10.1007/s00401-018-01956-z
- Xia, F., Ha, Y., Shi, S., Li, Y., Li, S., Luisi, J., et al. (2021). Early alterations of neurovascular unit in the retina in mouse models of tauopathy. *Acta Neuropathol. Commun.* 9:51. doi: 10.1186/s40478-021-01149-y

Conflict of Interest: The authors declare that the research was conducted in the absence of any commercial or financial relationships that could be construed as a potential conflict of interest.

Publisher's Note: All claims expressed in this article are solely those of the authors and do not necessarily represent those of their affiliated organizations, or those of the publisher, the editors and the reviewers. Any product that may be evaluated in this article, or claim that may be made by its manufacturer, is not guaranteed or endorsed by the publisher.

Copyright © 2021 Veys, Devroye, Lefevre, Cools, Vandenabeele and De Groef. This is an open-access article distributed under the terms of the Creative Commons Attribution License (CC BY). The use, distribution or reproduction in other forums is permitted, provided the original author(s) and the copyright owner(s) are credited and that the original publication in this journal is cited, in accordance with accepted academic practice. No use, distribution or reproduction is permitted which does not comply with these terms.